J Soils Sediments (2016) 16:1670–1679
DOI 10.1007/s11368-016-1356-y

SEDIMENTS, SEC 3 • HILLSLOPE AND RIVER BASIN SEDIMENT DYNAMICS • RESEARCH ARTICLE

An improved method for tracing soil erosion using rare earth elements

Gang Liu[1,2] **· Hai Xiao**[1] **· Puling Liu**[1] **· Qiong Zhang**[1] **· Jiaqiong Zhang**[1]

Received: 25 June 2015 / Accepted: 8 January 2016 / Published online: 25 January 2016

Abstract
Purpose The use of rare earth elements (REEs) as tracers provides a high-precision method for quantitative determinations of soil particle movement in soil erosion studies. In this study, a new calculation method was developed and tested to improve the precision of the REE tracing method and to expand the application of this method to areas with coarse-textured soils.
Materials and methods This study used purple soil to simulate a catchment with data based on a field survey of a small catchment located in the Three Gorges Area in China. Eight different powdered rare earth oxides, which included La_2O_3, CeO_2, Nd_2O_3, Sm_2O_3, Eu_2O_3, Tb_4O_7, Ho_2O_3 and Yb_2O_3, were applied as tracers to describe soil movement in this scaled catchment during three simulated rainfall events of 1.0, 1.5 and 2.0 mm min^{-1} rainfall intensity. Leaching experiments were conducted to investigate the vertical migration of REEs in soil layers. Particle size distributions (PSDs) and REE concentrations for each soil particle size class (1–2, 0.5–1, 0.25–0.5, 0.1–0.25, 0.075–0.1, 0.05–0.075, 0.02–0.05, 0.005–0.02 and <0.005 mm) were analysed to evaluate the precision of the proposed calculation method.
Results and discussion Most REEs remained in the first layer during leaching. The scanning electron microscopy-energy dispersive X-ray (SEM-EDX) mapping images showed that more REEs were adsorbed by small particles (≤0.1 mm), with large specific surface areas, than by large particles (>0.1 mm). During the three rainfall events, the coarsest size classes (1–2 and 0.5–1 mm) of the sediment samples were less than that of the soil. In contrast, the other classes, including <0.075 mm, showed the strongest adsorption for REEs, and the weight percentage of grains in eroded sediment was more than that in the source soil. The accuracy of the new proposed calculation method increased by 24.37, 20.25 and 3.84 % for the first, second and third storm, respectively, compared with the uncorrected mass of soil loss from the scaled catchment.
Conclusions The REEs bonded well with purple soil particles and the leaching of REEs from the tagged layer to the lower layers was minimal. The <0.075-mm particle size class had the strongest adsorption capacity for REEs. The soil loss estimates were improved with the new calculation method.

Keywords Coarse-textured soils · Erosion processes · Particle size distribution · Quantitative information · Sediment sources · Tracers

1 Introduction

To understand the spatial distribution of erosion and sediment sources, tracing techniques have been developed and applied. A number of tracers, such as ^{137}Cs (e.g. Koiter et al. 2013), $^{210}Pb_{ex}$ (e.g. Belmont et al. 2014), ^{7}Be (e.g. Liu et al. 2011), ^{60}Co (e.g. Greenwood et al. 2014), ^{59}Fe (e.g. Wooldridge 1965), glass particles (e.g. Young and Holt 1968) and rare earth elements (REEs) (e.g. Mahler et al. 1998) have been used. Of the fallout radioisotopes, ^{137}Cs has been most extensively used for studying soil erosion and deposition based on its accumulation and loss in various landscapes (Quine et al.

Responsible editor: Rajith Mukundan

✉ Gang Liu
gliu@foxmail.com

[1] State Key Laboratory of Soil Erosion and Dryland Farming on the Loess Plateau, Northwest A&F University, Yangling 712100, China

[2] USDA-ARS National Sedimentation Laboratory, Oxford, MS 38655, USA

1999; Walling and He 1999). However, this technique is not suitable for the short-term evaluation of erosion and deposition rates or tracking the fate of eroded soils. Due to differences in depth distribution, the combination of ^{137}Cs, $^{210}Pb_{ex}$ and ^{7}Be has the potential for distinguishing rill and sheet erosion in sediment source areas (Wallbrink and Murray 1993; Whiting et al. 2001). The multiple-tracer technique, which is called the fingerprinting technique, can identify sediment sources. The selection of tracers and explanation of fingerprinting signatures with specific reference to geomorphic processes are still problematic (Belmont et al. 2014). The radioactive ions, such as ^{60}Co and ^{56}Fe, can be deliberately applied to trace soil erosion but have radiological risks to both users and the environment. Exotic particles, such as glass, may not bind well with soil particles and aggregates.

REEs are those with atomic numbers 57 to 71. These elements have similar chemical properties. REEs are ideal for use as soil tracers because they satisfy the following criteria: strong adsorption to soil particles, sensitivity to analysis, ease of measurement, low background concentration in soil, no interference with soil transport processes, chemical stability, low plant uptake and they are environmentally safe (Zhang et al. 2001; Spencer et al. 2011). Powdered rare earth oxides (REOs) are industrial products that are insoluble in water and other basic solvents (Michaelides et al. 2010). REOs have been successfully utilised as tracers in soil erosion studies, including sediment transport and the redistribution and deposition of eroded soil (e.g. Tian et al. 1994; Matisoff et al. 2001; Zhang et al. 2003; Polyakov et al. 2004, 2009; Kimoto et al. 2006a; Lei et al. 2006). Presently, relevant studies have primarily focused on soils with a high clay or silt content. One of the assumptions made in using REE tracing is that the particle size distribution (PSD) of the source and sediment materials are similar. This assumption is valid in fine-textured soil but may not be valid in coarse-textured soils because of the mixing and redistribution of the different soil particles during transport. Size selectivity of eroded sediment readily occurs on steep slopes, which cover more than 90 % of the Three Gorges Area in China (Shi et al. 2012a, b, c). The redistribution of soil particles may affect the calculation precision for tracing soil erosion in coarse-textured soils because REEs with different size fractions possess different adsorption characteristics (Zhang et al. 2001; Kimoto et al. 2006b). Zhang et al. (2001) reported that the oxides preferentially bond with the soil particles <0.053 mm in fine-textured soil. Kimoto et al. (2006b) found REOs bond well with soil particles <0.09 mm in coarse-textured soil. Kimoto et al. (2006b) improved the accuracy by 4 % in the estimation of the total soil loss when sediment sorting occurred. However, their study used the assumed concentration of each particle size group in both parent soil and sediment instead of actual ones. Therefore, the precision of the REE technique in tracing soil erosion for coarse-textured soils still needs improvement.

This study aimed to develop and test a calculation method that takes into account the PSD during erosion processes, the vertical leaching of REEs and the adsorptive capacity of the different size fractions of soils. Results should not only improve the precision of the REE tracing method in soil erosion studies but should also expand the application of this method to areas with coarse-textured soils.

2 Materials and methods

2.1 Soil preparation

The upper 20 cm of a cultivated purple soil in a small catchment of Wangjiaqiao in Zigui County of Hubei Province in China (31°12′ N to 31°15′ N, 110°40′ E to 110°43′ E) was sampled for REE content. The soil was derived from sandy shale in a subtropical climate with mean temperatures between 11 and 18 °C. The average annual precipitation is 1016 mm, of which 70 % occurs between May and September. The soil had a bulk density and organic content of 1.3 g cm^{-3} and 0.97 %, respectively, and consisted of 1.97 % clay (<0.002 mm), 19.53 % silt (0.002 to 0.05 mm) and 78.50 % sand (0.05 to 2 mm). The soil is classified as an entisol according to the soil taxonomy of the US Department of Agriculture and covers approximately 78.7 % of the land area in the Three Gorges Area in China (Shi et al. 2009).

Eight different powdered REOs, which included La_2O_3, CeO_2, Nd_2O_3, Sm_2O_3, Eu_2O_3, Tb_4O_7, Ho_2O_3 and Yb_2O_3, were chosen for this study. Selection was based on cost considerations, amount required and analytical detection methodology (Liu et al. 2004). The physical properties and applied mass values of the REOs are listed in Table 1. Each of the powdered oxides was evenly mixed into separate soil samples (Liu et al. 2004).

2.2 Leaching experiment

A plastic tube, 7.5 cm in diameter and 16 cm in height, was cut into seven segments. The top 1-cm segment contained soil mixed with the selected REOs. The air-dried original soil was crushed to pass a 2-mm sieve and then placed into the plastic tube in segments from 1 to 2, 2 to 3, 3 to 4, 4 to 5, 5 to 9 and 9 to 14 cm. The plastic tube was covered by gauze at the bottom to allow for drainage. The tagged and original soils were carefully packed in the tube so that the bulk density of each layer of soil approximated field conditions. Deionised water was leached through the tubes for 48 h. Three replicates were used for each REO determination. Once leaching was completed, each segment was carefully removed. The soils were then dried and ground for extraction and analysis.

Table 1 Parameters required for the application of rare earth element (REE) oxides as tracers to an erosion study in a scaled catchment, Three Gorges Area, China

Parameters	Rare earth element oxides							
	La_2O_3	Yb_2O_3	CeO_2	Sm_2O_3	Eu_2O_3	Tb_4O_7	Nd_2O_3	Ho_2O_3
Molecular weight	325.84	394.08	172.13	348.72	351.91	747.70	336.47	277.86
Purity (%)	99.99	99.99	99.99	99.95	99.99	99.99	99.50	99.95
Average grain diameter (μm)	4.23	4.54	4.26	4.35	4.86	4.89	4.65	4.25
Particle density (g cm^{-3})	6.51	9.17	7.13	7.54	7.42	8.33	7.24	8.54
Background concentration of REOs (mg kg^{-1})	24.12	1.87	41.23	4.23	0.76	0.55	12.99	0.59
REO application concentration (mg kg^{-1})	858.6	89.2	1423.8	143.2	12.3	5.3	505.2	13.4
REO application mass (g)	283.18	29.86	553.21	54.69	3.94	1.62	100.48	2.76
REE number	I	II	III	IV	V	VI	VII	VIII
Landform type	Upstream upper slopes	Upstream lower slopes	Downstream upper slopes	Downstream lower slopes	Upper main gully	Lower main gully	Upper branch gullies	Lower branch gullies

2.3 Simulated rainfall experiment

Based on the field survey data, a replica of the catchment at a scale of 1:100 was constructed and subjected to simulated rainfall in the testing facilities of the China Three Gorges University. The catchment boundary was demarcated by a brick and concrete wall. The bottom was filled with sand to facilitate drainage. The top 10 cm was evenly filled with purple soil mixed with REOs at an average bulk density of 1.3 g cm^{-3}. Eight soil samples containing the different REE oxides (number I to VIII) were applied separately to eight different landform types that were potential sediment source areas, distributed across the catchment at 14 zones. A schematic of the scaled catchment and distribution of the eight REOs in various zones is shown in Fig. 1. The experimental area was approximately 20 m^2. The elevations of the highest and lowest positions were about 1.3 and 0.4 m, respectively. The catchment had one main gully and two branch gullies. The main gully was 5.5-m long from its highest position to the catchment outlet. The gradients of the bed and banks of the upper half of the main gully ranged from 10° to 15° and from 20° to 35°, respectively. The gradients of the bed and banks of the lower half of the gully ranged from 0° to 5° and from 15° to 30°, respectively. The two sides of the main gully each had one branch gully. The left and right gullies were 2.2 and 1.9 m long, respectively; the gradients of both gully beds ranged from 0° to 10°, while those of their banks ranged from 25° to 35° and 15° to 30°, respectively. The gradients on the lower and upper slopes ranged from 0° to 10°. The catchment surface was then smoothed, watered, covered with a plastic sheet and left undisturbed for 3 months to enhance the binding of the REEs to the soil particles.

The rainfall simulator, consisting of nine sets of three nozzles each, was positioned above the experimental area at a height of 6 m. The simulator sprayed tap water (sodium adsorption ratio = 1.94, electrical conductivity = 0.87 ds m^{-1}) uniformly over the plot area. Rain had a distribution uniformity of better than 86 %. Three rainstorms with intensities of 1.0, 1.5 and 2.0 mm min^{-1} and median raindrop diameters of 2.46, 3.18 and 3.54 mm, respectively, were simulated for 30 min. These intensities were based on the natural maximum rainfall intensity occurring for a 30-min period during moderate and heavy rainstorms in the study region. Runoff and sediments were collected sequentially in plastic containers at intervals of 2 min throughout the storms. The volume of water in each container was measured, and the sediment was air dried and weighed. The catchment area was covered with a plastic sheet after every rainfall event and left undisturbed until the next rainfall event, 3 days later.

2.4 Laboratory analysis

A method for the extraction of metals from environmental samples was used to extract the REEs in soil and sediment samples (Zhang et al. 2001). The mean of three soil sample replicates was used in all analyses. The samples were analysed by inductively coupled plasma mass spectrometry (ICP-MS X Series 2, Thermo Fisher Scientific, US) at the College of Chemistry and Life Science, China Three Gorges University. An aliquot of a stock internal standard solution containing Rh and Re (10 μg L^{-1}) was added to the tube. Three replicate measurements of REEs from

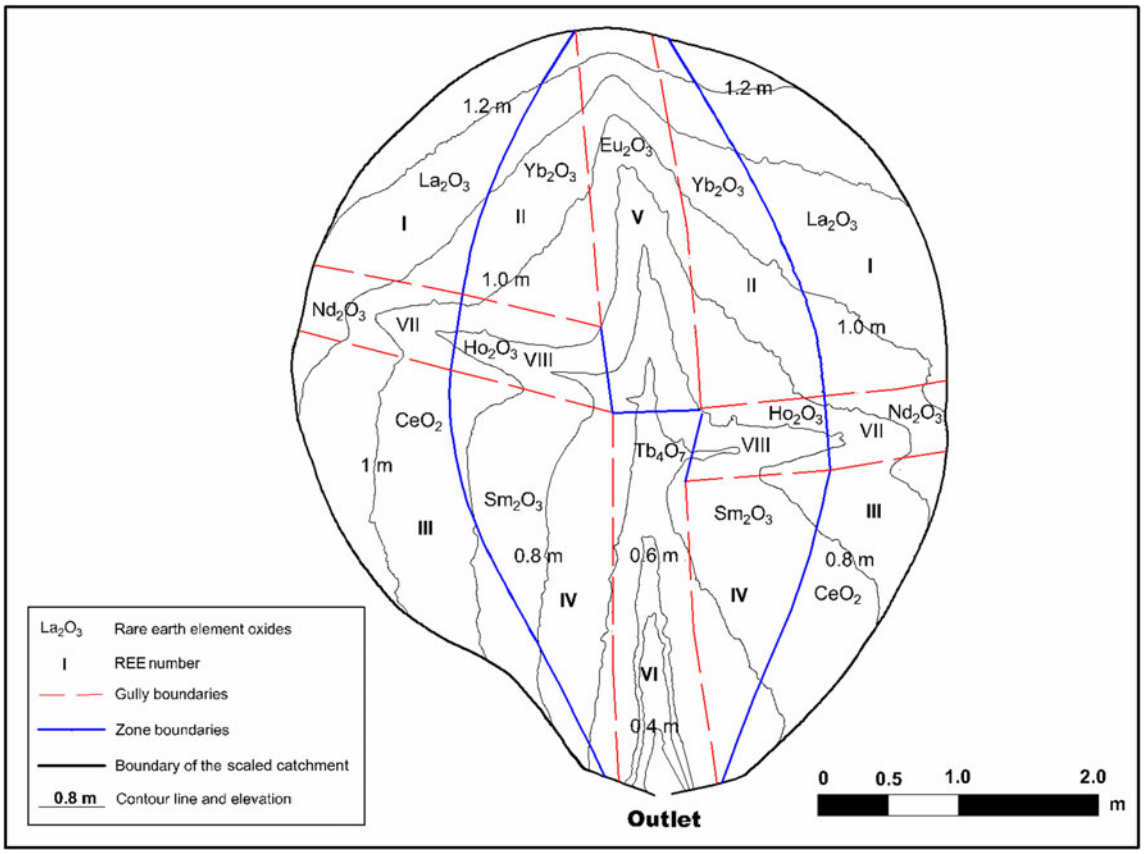

Fig. 1 Schematic of the scaled catchment. Eight rare earth element oxides (I to VIII) were applied to eight landform types distributed in 14 zones across the catchment. The upstream upper and lower slopes received La_2O_3 (REE I) and Yb_2O_3 (REE II), respectively. The downstream upper and lower slopes had CeO_2 (REEIII) and Sm_2O_3 (REE IV) applied, respectively. The upper and lower parts of the main gully had Eu_2O_3 (REE V) and Tb_4O_7 (REE VI) applied, respectively. The upper and lower parts of the branch gullies had Nd_2O_3 (REE VII) and Ho_2O_3 (REE VIII) applied, respectively

each extracted sample were made. The particle size fractions of soil and sediment were separated and analysed by the standard method of dry sieving and centrifugation of the sample (Stemmer et al. 1998; Lv et al. 2012). The distribution of REEs in the samples was characterised by a scanning electron microscopy (SEM, JSM-7500 F, JEOL, Japan) at an accelerating voltage of 10 kV using a EVO LS 25 (Zeiss, Germany). Energy dispersive X-ray (EDX) was undertaken with an X-ray detector (INCA X-act, Oxford instruments, UK).

2.5 Data processing

The mass of soil loss from a given REE j (j=I, II, III, …, VIII) region in the catchment was calculated using the relationship:

$$w_j = \frac{(R_j - B_j) \times W}{C_j} \quad (1)$$

where w_j is the mass of soil loss from region j (kg); R_j is the actual measured concentration of REEs in the sediment samples of region j (mg kg^{-1}); B_j is the background concentration of REEs in the soil of region j (mg kg^{-1}); W is the mass of the sediment samples (kg); and C_j is the added concentration of REEs in region j (mg kg^{-1}). Experimental error was estimated by:

$$\sigma = \left(\frac{\sum_{j=\mathrm{I}}^{\mathrm{VIII}} w_j}{W} - 1 \right) \times 100\% \quad (2)$$

where σ is the experimental error estimated by comparing the actual and calculated masses of soil loss.

To improve the calculation accuracy in tracking soil erosion, the differences in adsorption capacity among the soil particle size classes were considered. Parameters Q_{ij} and q_{ij} were assumed to be the concentration of REEs (mg kg^{-1}) applied in the region j in particle size class i (i=1, 2, 3,…, 9, representing the nine classes, 1–2, 0.5–1, 0.25–0.5, 0.1–0.25, 0.075–0.1, 0.05–0.075, 0.02–0.05, 0.005–0.02 and <0.005 mm) for tagged soil and sediment, respectively; Q_j and q_j are the concentrations of added REEs (mg kg^{-1}) to region j for tagged soil and sediment;

S_{ij} and s_{ij} are the masses of added REEs (kg) to region j in size class i for tagged soil and sediment; M_i and m_i are the masses of soil particle size class i (kg) for tagged soil and sediment; S_j and s_j are the masses of added REEs (kg) to region j for tagged soil and sediment; and K_j is the correction factor of added REEs to region j. Thus:

$$Q_{ij} = \frac{S_{ij}}{M_i} \tag{3}$$

$$q_{ij} = \frac{s_{ij}}{m_i} \tag{4}$$

$$K_j = \frac{q_j}{Q_j} \tag{5}$$

The following hypothesis is proposed: Q_{ij} is equal to q_{ij} because of the strong adsorption of REEs by soil particles (Mahler et al. 1998; Zhang et al. 2001; Kimoto et al. 2006b). According to Eqs. 3, 4 and 5, K_j is given by:

$$K_j = \frac{\sum_{i=1}^{9} \frac{m_i}{M_i} S_{ij}}{\sum_{i=1}^{9} S_{ij}} \tag{6}$$

The corrected concentration of REEs in region j of the sediment samples (R_j', $\mathrm{mg \cdot kg^{-1}}$) can be estimated by:

$$R_j' = K_j \times R_j \tag{7}$$

The corrected mass of soil loss in region j (w_j', kg) can be calculated from:

$$w_j' = \frac{\left(R_j' - B_j\right) \times W}{C_j} \tag{8}$$

The experimental error estimated by comparing the actual and corrected mass of soil loss (σ') can be estimated by:

$$\sigma' = \left(\frac{\sum_{j=1}^{\mathrm{VIII}} w_j'}{W} - 1 \right) \times 100\% \tag{9}$$

3 Results and discussion

3.1 REE concentrations for leached soil layers

Figure 2 shows the extracted REE concentrations for each leached soil layer. The REE concentrations for the first layer (0–1 cm) were the highest. The REE concentrations for the second layer (1–2 cm) were slightly higher than those of the deeper layers. However, these concentrations were not as high as those of the first layer, which indicates minimal leaching into the second layer. Below the second layer, the REE concentrations were not noticeably different from the background concentrations in the soil (Table 1). These results indicate that most REEs remained in the first layer during leaching suggesting that the REEs were firmly attached to the soil particles of the purple soils. Therefore, the leaching of the REEs from the tagged layer into the lower layers was minimal.

3.2 REE concentrations for different soil particle size classes

Figure 3 shows the typical SEM-EDX mapping images of soil samples mixed with REEs. The distribution of colour dots indicated that different REEs were preferentially adsorbed by soil particles of different sizes. The concentration of dots (REEs) was densest on soil particles <0.1 mm. However, a large number of observations also suggested that more REEs were absorbed by smaller particles (≤0.1 mm) with larger specific surface area (Yang et al. 2013) than larger particles (>0.1 mm). However, this qualitative analysis was not able to provide a quantitative distribution of REEs in soil particles of different sizes and also failed to show differences in concentration among REEs in particles of the same size.

The concentrations of the eight kinds of REEs for the nine particle size classes in parent soil and sediment samples from three simulated rainstorms are shown in Table 2. These data indicate that the concentration of seven elements (i.e. Ce, La, Nd, Sm, Ho, Eu and Tb) increased to a peak value with decreasing soil particle size from 2 to 0.005 mm but decreased for the size class <0.005 mm. The element Yb was very rare in size classes >0.075 mm, but increased to a peak value in classes 0.05–0.075 mm, and then gradually decreased in the smaller particle size classes. Although the concentrations of the eight elements significantly differed in each soil particle size class, the REE concentration in classes <0.075 mm were clearly larger than those in the size classes 2–0.075 mm. Therefore, the particle size of <0.075 mm appears to have the strongest adsorption capacity for REEs of this purple soil. This result is consistent with the findings of other studies and is likely related to the distribution of soil particle size with the mineralogy of the clays (Mahler et al. 1998; Zhang et al. 2001; Kimoto et al. 2006b). However, the differences in the concentrations of REEs for most particle size classes in both parent soil and sediment were not significantly different (Table 2). The only significant differences were for Yb and Ho in the

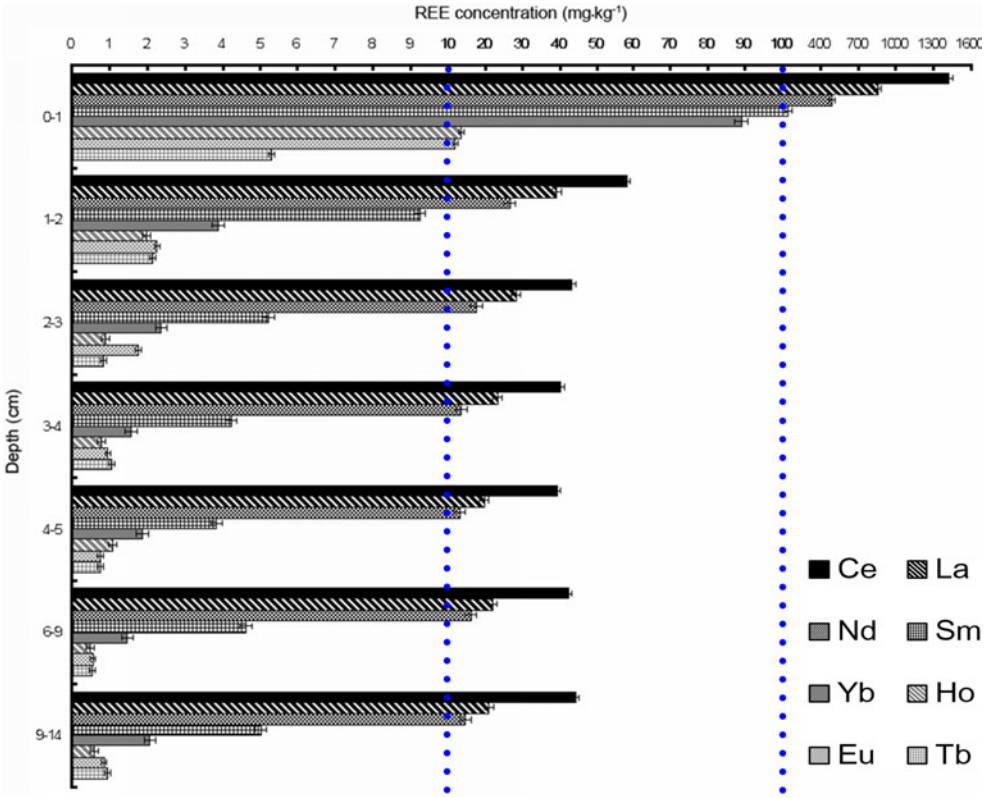

Fig. 2 Mean rare earth element (REE) concentration for each leached soil layer (1–2, 2–3, 3–4, 4–5, 5–9 and 9–14 cm). *Error bars* show standard deviations for replicate samples ($n = 3$)

coarse classes (1–2 mm and 0.5–1 mm). The concentrations of these REEs in these two classes were very low, compared with the fine classes. The differences would hardly affect the calculations using Eqs. 6, 7, 8 and 9. Therefore, our hypothesis—that the concentrations of REEs for different particle size classes in both parent soil and sediment are the same—is acceptable.

3.3 PSD of soil and sediment samples

During the three rainfall events, sediment samples were collected continuously at 6-min intervals. The PSDs of the soil and sediment samples were determined and the results are shown in Table 3. These data show that the coarsest size classes (1–2 and 0.5–1 mm) of the sediment samples had smaller

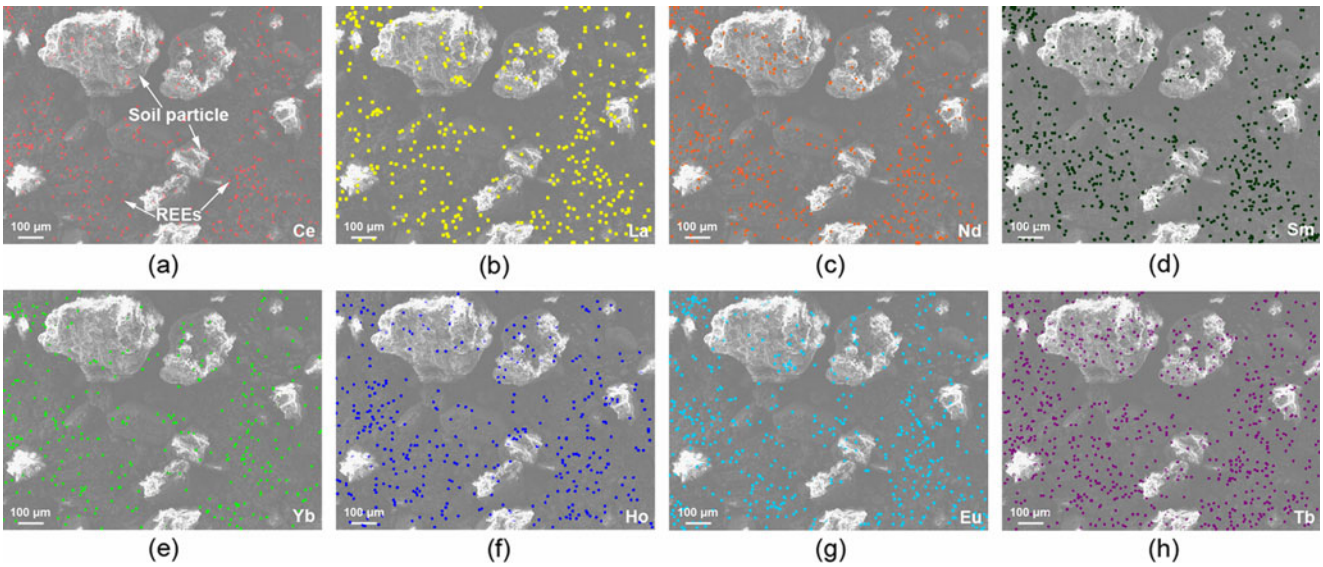

Fig. 3 SEM-EDX mapping images of the eight kinds of rare earth element (REE) mixed in parent soil, **a** Ce, **b** La, **c** Nd, **d** Sm, **e** Yb, **f** Ho, **g** Eu and **h** Tb, adsorbed by soil particles of different sizes. REEs are indicated by *coloured dots*

Table 2 Mean rare earth element (REE) concentration for each particle size class in parent soil and sediment samples from three simulated rainstorms

Particle size (mm)	Samples	Rare earth element concentration (mg kg^{-1})[a]							
		Ce	La	Nd	Sm	Yb	Ho	Eu	Tb
1–2	Parent soil	58.2 ± 0.9	66.8 ± 0.7	3.8 ± 0.4	6.0 ± 0.2	1.9 ± 0.1a	0.6 ± 0.0a	3.2 ± 0.1	4.9 ± 0.7
	Sediment 1	56.7 ± 0.6	65.9 ± 0.6	4.5 ± 0.5	6.3 ± 0.3	1.5 ± 0.1b	0.7 ± 0.1ab	3.3 ± 0.2	4.7 ± 0.6
	Sediment 2	58.1 ± 1.0	66.3 ± 0.5	3.7 ± 0.4	5.9 ± 0.4	2.2 ± 0.2c	0.8 ± 0.1b	3.1 ± 0.1	5.3 ± 0.8
	Sediment 3	57.8 ± 0.7	67.0 ± 0.7	4.3 ± 0.5	6.4 ± 0.2	1.7 ± 0.1ab	0.6 ± 0.0a	3.1 ± 0.1	5.1 ± 0.7
0.5–1	Parent soil	105.6 ± 1.6	142.3 ± 1.4	4.4 ± 0.5	7.6 ± 0.3	3.3 ± 0.1a	1.1 ± 0.1	5.1 ± 0.2	8.1 ± 1.2
	Sediment 1	107.3 ± 1.9	140.5 ± 1.3	5.1 ± 0.6	7.7 ± 0.3	3.1 ± 0.1b	1.2 ± 0.1	5.2 ± 0.3	7.5 ± 1.1
	Sediment 2	104.4 ± 1.4	142.1 ± 1.6	4.8 ± 0.5	7.8 ± 0.4	3.5 ± 0.1c	1.2 ± 0.1	4.8 ± 0.1	7.9 ± 1.2
	Sediment 3	107.1 ± 1.7	139.8 ± 1.2	4.2 ± 0.4	7.2 ± 0.3	3.4 ± 0.1ac	1.3 ± 0.2	4.8 ± 0.2	8.7 ± 1.4
0.25–0.5	Parent soil	90.1 ± 1.4	168.8 ± 1.7	5.1 ± 0.6	8.3 ± 0.3	2.0 ± 0.1	0.9 ± 0.0	4.7 ± 0.2	7.6 ± 1.1
	Sediment 1	89.1 ± 1.2	169.7 ± 1.8	5.5 ± 0.7	7.9 ± 0.2	2.0 ± 0.1	0.8 ± 0.0	4.8 ± 0.2	6.9 ± 1.0
	Sediment 2	91.4 ± 1.5	167.5 ± 1.5	4.6 ± 0.5	8.4 ± 0.3	2.2 ± 0.2	0.8 ± 0.0	4.6 ± 0.2	6.8 ± 0.9
	Sediment 3	91.8 ± 1.6	168.0 ± 1.6	4.8 ± 0.6	8.1 ± 0.3	2.1 ± 0.1	0.9 ± 0.0	5.0 ± 0.3	7.9 ± 1.1
0.1–0.25	Parent soil	136.4 ± 2.0	282.4 ± 2.8	3.5 ± 0.4	4.6 ± 0.2	2.6 ± 0.1	1.2 ± 0.1	5.7 ± 0.2	9.1 ± 1.4
	Sediment 1	133.9 ± 1.9	279.0 ± 2.7	4.2 ± 0.5	4.7 ± 0.2	2.6 ± 0.1	1.2 ± 0.1	5.7 ± 0.2	8.7 ± 1.4
	Sediment 2	134.1 ± 2.0	284.1 ± 2.8	3.9 ± 0.4	4.4 ± 0.2	2.5 ± 0.1	1.1 ± 0.1	5.8 ± 0.2	9.3 ± 1.4
	Sediment 3	137.8 ± 2.1	280.2 ± 2.7	3.6 ± 0.4	4.4 ± 0.2	2.5 ± 0.1	1.1 ± 0.1	5.9 ± 0.1	8.2 ± 1.3
0.075–0.1	Parent soil	204.8 ± 3.1	443.4 ± 4.1	45.8 ± 5.0	61.4 ± 2.5	3.6 ± 0.1	7.9 ± 0.4	8.0 ± 0.3	12.9 ± 1.9
	Sediment 1	199.4 ± 3.0	451.1 ± 4.2	44.7 ± 5.0	58.2 ± 2.4	3.5 ± 0.1	7.8 ± 0.5	7.8 ± 0.3	11.4 ± 1.8
	Sediment 2	205.0 ± 3.1	450.6 ± 4.1	42.3 ± 4.9	57.3 ± 2.4	3.6 ± 0.1	8.4 ± 0.4	7.7 ± 0.3	11.8 ± 1.8
	Sediment 3	201.6 ± 3.0	447.5 ± 4.0	43.3 ± 5.0	60.8 ± 2.5	3.5 ± 0.1	7.6 ± 0.4	8.2 ± 0.3	12.6 ± 1.9
0.05–0.075	Parent soil	816.6 ± 12.2	860.4 ± 8.6	156.2 ± 17.2	193.5 ± 7.7	606.4 ± 24.3	38.9 ± 1.9	14.8 ± 0.6	176.0 ± 26.4
	Sediment 1	807.4 ± 12.0	869.8 ± 8.7	164.6 ± 17.4	188.7 ± 7.5	617.2 ± 24.6	37.8 ± 1.8	14.1 ± 0.5	182.3 ± 27.2
	Sediment 2	823.5 ± 12.4	872.5 ± 8.8	159.4 ± 17.3	184.6 ± 7.4	608.7 ± 24.3	39.2 ± 1.9	14.9 ± 0.6	172.9 ± 25.9
	Sediment 3	826.6 ± 12.4	867.1 ± 8.6	167.0 ± 17.4	196.7 ± 7.8	614.2 ± 24.5	38.1 ± 1.8	15.2 ± 0.7	178.4 ± 26.6
0.02–0.05	Parent soil	2472.0 ± 37.1	3462.0 ± 34.6	462.2 ± 50.8	758.2 ± 30.3	436.4 ± 17.5	116.5 ± 5.8	314.6 ± 12.6	655.8 ± 48.4
	Sediment 1	2494.3 ± 38.6	3487.6 ± 34.8	483.7 ± 51.2	737.5 ± 29.7	458.4 ± 18.4	125.8 ± 6.0	317.6 ± 12.7	673.4 ± 49.1
	Sediment 2	2488.5 ± 37.7	3496.7 ± 35.1	454.8 ± 50.5	729.7 ± 29.4	447.0 ± 17.7	127.3 ± 6.4	322.9 ± 12.9	642.5 ± 48.8
	Sediment 3	2504.6 ± 38.8	3510.1 ± 35.4	479.0 ± 50.3	781.4 ± 31.5	427.6 ± 16.9	122.4 ± 5.9	338.3 ± 13.2	688.7 ± 49.4
0.005–0.02	Parent soil	3088.0 ± 46.3	7120.0 ± 71.2	594.4 ± 65.4	1049.4 ± 42.0	259.6 ± 10.4	129.0 ± 6.5	574.4 ± 23.0	876.8 ± 71.5
	Sediment 1	3127.2 ± 47.2	7106.9 ± 70.8	611.8 ± 66.1	1088.3 ± 43.3	248.6 ± 10.1	136.5 ± 6.9	558.7 ± 22.6	852.3 ± 70.8
	Sediment 2	3056.9 ± 45.9	7222.5 ± 72.3	573.5 ± 64.9	1123.6 ± 44.1	265.6 ± 11.8	125.4 ± 6.4	562.3 ± 22.8	868.7 ± 71.0
	Sediment 3	3114.1 ± 46.8	7208.7 ± 71.8	605.3 ± 65.8	1095.0 ± 43.1	264.6 ± 11.3	133.2 ± 6.7	579.9 ± 23.1	884.0 ± 72.1
<0.005	Parent soil	555.0 ± 8.3	2901.0 ± 29.0	212.9 ± 23.4	171.1 ± 6.8	9.7 ± 0.4	20.4 ± 1.0	38.4 ± 1.5	32.3 ± 4.8
	Sediment 1	547.5 ± 7.9	2893.4 ± 28.9	226.7 ± 23.6	168.9 ± 6.7	9.1 ± 0.4	21.2 ± 1.3	36.9 ± 1.3	31.4 ± 4.6
	Sediment 2	555.3 ± 8.8	2911.0 ± 29.1	218.3 ± 23.5	166.7 ± 6.6	8.8 ± 0.3	20.9 ± 1.2	37.2 ± 1.3	33.5 ± 5.0
	Sediment 3	562.3 ± 9.1	2918.0 ± 29.2	209.5 ± 23.4	173.6 ± 6.8	10.2 ± 0.4	22.3 ± 1.5	37.9 ± 1.4	33.0 ± 4.9

[a] Fisher's LSD was used to test for differences between means. Means followed by the different letters within a variable in the same row indicate significant differences at $\alpha = 0.05$ in every group

mass fractions than the original soil. In contrast, the other classes, including <0.075 mm, showed the strongest adsorption for REEs (Table 3), and the weight percentage of grains in sediment was larger than that in the soil. Also, the fact that the PSDs of the sediment samples did not noticeably change during the three rainstorm events may be due to the short transport distance and absence of vegetation. Therefore, the size selectivity of eroded sediment was continuous and stable. Shi et al. (2012a, b, c) found that selective transport of fine sediment and selective deposition of coarse sediment occurred mainly on steep slopes and, to a lesser degree, elsewhere in a natural watershed. However, the complicated flow discharge processes and long transport distance of sediment in natural catchments may cause size selectivity processes of eroded sediment to be more complex than that in a scaled catchment.

3.4 Calculation of soil loss and error analysis

Considering the differences in the adsorption capacity for REEs among the soil particle classes (Table 2) and in PSD

Table 3 Particle size distribution of soil and sediment samples from the scaled catchment during three simulated rainstorms

Particle size (mm)	Soil samples (%)	Sediment samples (%)														
		Rainfall duration (min) for intensity of 1.0 mm min^{-1}					Rainfall duration (min) for intensity of 1.5 mm min^{-1}					Rainfall duration (min) for intensity of 2.0 mm min^{-1}				
		1–6	7–12	13–18	19–24	25–30	1–6	7–12	13–18	19–24	25–30	1–6	7–12	13–18	19–24	25–30
1–2	12.91	7.25	6.86	10.16	6.86	7.11	9.89	6.98	7.57	10.22	6.78	7.73	10.04	6.74	7.75	9.53
0.5–1	35.50	32.64	31.98	30.51	30.95	31.02	29.30	30.56	29.63	28.87	28.04	28.40	28.79	24.41	28.20	28.43
0.25–0.5	18.55	20.80	21.88	20.40	20.10	21.80	22.14	19.67	22.53	22.29	22.43	22.64	22.47	24.10	22.84	22.86
0.1–0.25	13.74	12.58	16.54	15.84	15.54	16.60	15.82	17.04	16.90	15.82	17.14	17.48	15.96	18.76	17.43	16.21
0.075–0.1	5.04	6.57	6.14	6.41	6.70	6.21	6.37	6.66	6.26	6.60	6.81	6.68	6.66	6.99	6.88	6.83
0.05–0.075	9.88	12.73	11.18	11.00	12.85	11.26	11.09	12.89	11.40	11.06	13.00	11.48	11.14	13.46	11.59	10.26
0.02–0.05	2.24	3.86	2.75	2.75	3.71	2.67	2.63	3.17	2.60	2.52	2.97	2.59	2.49	2.87	2.53	2.46
0.005–0.02	1.85	2.65	2.65	2.34	2.43	2.57	2.23	2.25	2.48	2.15	2.20	2.40	2.02	2.06	2.25	1.99
<0.005	0.29	0.92	0.73	0.59	0.86	0.69	0.54	0.80	0.62	0.47	0.63	0.59	0.43	0.61	0.52	0.41

among the sediment and soil samples (Table 3), the corrected soil loss and error during the three rainstorm events were calculated using Eqs. 1, 6, 7, 8 and 9 (Table 4). The uncorrected soil loss and error were calculated using Eqs. 1 and 2. The uncorrected amount of soil loss was larger than both the corrected and the collected amount of sediment during the three rainstorm events. During the three rainstorm events of 1.0, 1.5 and 2.0 mm min^{-1}, the errors in the uncorrected amount were 19.57–57.14 %, 12.84–40.00 % and 9.50–37.27 %, respectively. These values were 8.24–13.64 %, 3.03–10.54 % and 4.55–23.83 %, respectively, for the corrected amount of soil loss during the three rainfall events. The amounts of calculated soil loss were overestimated by using the uncorrected calculation method. After correction, the errors for estimating the amount of soil loss were reduced to 9.78–46.94 %, 8.78–29.46 % and 2.51–13.44 % for the

Table 4 Calculation errors of corrected and uncorrected amounts of soil loss from the scaled catchment during three simulated rainstorms

Rainfall intensity (mm min^{-1})	Rainfall duration (min)	Uncorrected amount of soil loss (kg) Eq. 1	Corrected amount of soil loss (kg) Eqs. 1, 6, 7, 8	Amount of collected sediment (kg)	Error of uncorrected mass (%) Eq. 2	Error of corrected mass (%) Eq. 9	Reduction of error (%)
1.0	0–6	0.77	0.54	0.49	57.14	10.20	46.94
	7–12	1.02	0.75	0.66	54.55	13.64	40.91
	13–18	1.12	0.92	0.85	31.76	8.24	23.53
	19–24	1.32	1.15	1.02	29.41	12.75	16.67
	25–30	1.10	1.01	0.92	19.57	9.78	9.78
	0–30	5.33	4.37	3.94	35.28	10.91	24.37
1.5	0–6	6.51	5.14	4.65	40.00	10.54	29.46
	7–12	8.42	6.81	6.61	27.38	3.03	24.36
	13–18	5.56	4.66	4.49	23.83	3.79	20.04
	19–24	5.52	4.77	4.60	20.00	3.70	16.30
	25–30	5.01	4.62	4.44	12.84	4.05	8.78
	0–30	31.02	26.00	24.79	25.13	4.88	20.25
2.0	0–6	6.74	6.08	4.91	37.27	23.83	13.44
	7–12	6.66	6.44	5.53	20.43	16.46	3.98
	13–18	6.35	6.21	5.58	13.80	11.29	2.51
	19–24	6.09	5.94	5.51	10.53	7.80	2.72
	25–30	5.53	5.28	5.05	9.50	4.55	4.95
	0–30	31.37	30.35	26.58	18.02	14.18	3.84

first, second and third storm, respectively. For the three rainstorms, the errors of corrected mass were 10.91, 4.88 and 14.18 %, respectively. These values were similar or lower than those in the experiment on loessial soil (Liu et al. 2004; Li et al. 2006), which had high clay and silt contents. Furthermore, the corrected calculation accuracy increased by 24.37, 20.25 and 3.84 % compared with the uncorrected mass. The lower improvement for the third rainfall event may be caused by the reduced finer particles (<0.075 mm) in the sediment (Table 3).

Although the accuracy of soil loss estimate was improved in a scaled catchment, the accuracy may be reduced by numerous factors in a natural watershed because of the spatial and temporal complexity of runoff and erosion processes (Shi et al. 2012b; Belmont et al. 2014). For instance, flood discharge processes are more complicated at a larger scale than at a smaller scale. Complicated flood discharge processes result in complex sediment transport, deposition and size selectivity processes (Shi et al. 2012b; Belmont et al. 2014). Therefore, before being transported out of the watershed, REEs may be redistributed several times by detachment, transport and deposition followed by resuspension in runoff. The accuracy of the soil loss calculation would be low if we measure only the REE concentration in the sediment from the watershed outlet. Thus, to improve the application accuracy of the REE tracing method in the field, automatic sampling systems within the natural watershed could be used to provide more detailed information on flow, sediment transport and deposition, especially on REE redistribution, in real time during rainstorms. Furthermore, the pointing or sectioning distribution method of applying REEs should be used to reduce the cost and minimise soil surface disturbance (Liu et al. 1997).

4 Conclusions

Leaching experiments were conducted to investigate the vertical migration of REEs in soil layers. Results indicated that REEs bond well with purple soil particles and that REE leaching from the tagged layer to the lower layers was minimal.

A rainfall simulation study was conducted to estimate the soil loss from a scaled catchment. During three rainstorm events of 1.0, 1.5 and 2.0 mm min^{-1}, the PSDs of the sediments were very different from that of the soil. The former had a lower content of the coarsest classes (1–2 and 0.5–1 mm) but higher content of other classes, including <0.075 mm, which had the strongest adsorption capacity for REEs. In this study, the size selectivity of eroded sediment was clear.

New calculation formulae were developed to estimate soil loss from the watershed. These formulae consider the differences in adsorption ability for REEs among soil particle classes and the PSDs among the sediment and parent soil samples. Data from this simulated rainfall experiment were used to prove that the new formulae improved the accuracy of the soil loss calculation by using REEs as tracers. However, additional work is needed to apply the approach described in this work to the investigation of soil erosion, transport and deposition in a natural watershed.

Acknowledgments We thank the editors and two anonymous reviewers for their valuable comments on the manuscript, and we thank Dr. Glenn Wilson for his suggestions and improving the English writing of the manuscript. This research was jointly supported by the National Natural Science Foundation of China (No. 41201270), the National Key Technology Research and Development Program of the Ministry of Science and Technology of China (No. 2015BAC01B03), the West Light Foundation of The Chinese Academy of Sciences (No. 2014-91), the Shaanxi Science and Technology Co-ordination Innovation Engineering Project (No. 2013KTDZ03-03-01), the Scientific Research Foundation of Northwest A&F University (No. 2013BSJJ082) and China Scholarship Council (No. 201404910141).

References

Belmont P, Willenbring JK, Schottler SP, Marquard J, Kumarasamy K, Hemmis JM (2014) Toward generalizable sediment fingerprinting with tracers that are conservative and nonconservative over sediment routing timescales. J Soils Sediments 14:1479–1492

Greenwood P, Walling DE, Quine TA (2014) Using caesium-134 and cobalt-60 as tracers to assess the remobilization of recently-deposited overbank-derived sediment on river floodplains during subsequent inundation events. Earth Surf Process Landf 39:228–244

Kimoto A, Nearing MA, Shipitalo MJ, Polyakov VO (2006a) Multi-year tracking of sediment sources in a small agricultural watershed using rare earth elements. Earth Surf Process Landf 31:1763–1774

Kimoto A, Nearing MA, Zhang XC, Powell DM (2006b) Applicability of rare earth element oxides as a sediment tracer for coarse-textured soils. Catena 65:214–221

Koiter AJ, Lobb DA, Owens PN, Petticrew EL, Tiessen KHD, Li S (2013) Investigating the role of connectivity and scale in assessing the sources of sediment in an agricultural watershed in the Canadian prairies using sediment source fingerprinting. J Soils Sediments 13:1676–1691

Lei TW, Zhang QW, Zhao J, Nearing MA (2006) Tracing sediment dynamics and sources in eroding rills with rare earth elements. Eur J Soil Sci 57:287–294

Li M, Li ZB, Ding WF, Liu PL, Yao WY (2006) Using rare earth element tracers and neutron activation analysis to study rill erosion process. Appl Radiat Isot 64:402–408

Liu PL, Tian JL, Zhou PH, Li YQ, Ju TJ (1997) Studies of operating techniques on REE tracer method applying to soil erosion. Res Soil Water Conserv 4:10–16

Liu PL, Tian JL, Zhou PH, Yang MY, Shi H (2004) Stable rare earth element tracers to evaluate soil erosion. Soil Tillage Res 76:147–155

Liu G, Yang MY, Warrington DN, Liu PL, Tian JL (2011) Using beryllium-7 to monitor the relative proportions of interrill and rill erosion from loessal soil slopes in a single rainfall event. Earth Surf Process Landf 36:439–448

Lv HJ, He HB, Zhang XD (2012) The options of conditions on ultrasonic dispersion and centrifugal separation in soil particle size fractionation. Chin J Soil Sci 43:1126–1130

Mahler BJ, Bennett PC, Zimmerman M (1998) Lanthanide-labeled clay: a new method for tracing sediment transport in Karst. Ground Water 36:835–843

Matisoff G, Ketterer ME, Wilson CG, Layman R, Whiting PJ (2001) Transport of rare earth element-tagged soil particles in response to thunderstorm runoff. Environ Sci Technol 35:3356–3362

Michaelides K, Lbraim L, Nord G, Esteves M (2010) Tracing sediment redistribution across a break in slope using rare earth elements. Earth Surf Process Landf 35:575–587

Polyakov VO, Nearing MA, Shiptalo MJ (2004) Tracking sediment redistribution in a small watershed: implications for agro-landscape evolution. Earth Surf Process Landf 29:1275–1291

Polyakov VO, Kimoto A, Nearing MA, Nichols MH (2009) Tracing sediment movement on a semiarid watershed using rare earth elements. Soil Sci Soc Am J 73:1559–1565

Quine TA, Walling DE, Chakela QK, Mandiringana OT, Zhang X (1999) Rates and patterns of tillage and water erosion on terraces and contour strips: evidence from caesium-137 measurements. Catena 36: 115–142

Shi ZH, Chen LD, Cai CF, Li ZX, Liu GH (2009) Effects of long-term fertilization and mulch on soil fertility in contour hedgerow systems: a case study on steeplands from the Three Gorges Area, China. Nutr Cycl Agroecosyst 84:39–48

Shi ZH, Ai L, Fang NF, Zhu HD (2012a) Modeling the impacts of integrated small watershed management on soil erosion and sediment delivery: a case study in the Three Gorges Area, China. J Hydrol 438–439:156–167

Shi ZH, Fang NF, Wu FZ, Wang L, Yue BJ, Wu GL (2012b) Soil erosion processes and sediment sorting associated with transport mechanisms. J Hydrol 454–455:123–130

Shi ZH, Yue BJ, Wang L, Fang NF, Wang D, Wu FZ (2012c) Effects of mulch cover rate on interrill erosion processes and the size selectivity of eroded sediment on steep slopes. Soil Sci Soc Am J 77:257–267

Spencer KL, Suzuki K, Hillier S (2011) The development of rare earth element-labelled potassium-depleted clays for use as cohesive sediment tracers in aquatic environments. J Soils Sediments 11:1052–1061

Stemmer M, Gerzabek MH, Kandeler E (1998) Organic matter and enzyme activity in particle-size fractions of soils obtained after low-energy sonication. Soil Biol Biochem 30:9–17

Tian JL, Zhou PH, Liu PL (1994) REE tracer method for studies on soil erosion. Int J Sediment Res 9:39–46

Wallbrink PJ, Murray AS (1993) Use of fallout radionuclides as indicators of erosion processes. Hydrol Process 7:297–304

Walling DE, He Q (1999) Improved models for estimating soil erosion rates from cesium-137 measurements. J Environ Qual 28:611–622

Whiting PJ, Bonniwell EC, Matifoff G (2001) Depth and areal extent of sheet and rill erosion based on radionuclides in soils and suspended sediment. Geology 29:1131–1134

Wooldridge DD (1965) Tracing soil particle movement with Fe-59. Soil Sci Soc Am J 29:469–472

Yang MY, Walling DE, Sun XJ, Zhang FB, Zhang B (2013) A wind tunnel experiment to explore the feasibility of using beryllium-7 measurements to estimate soil loss by wind erosion. Geochim Cosmochim Acta 114:81–93

Young RA, Holt RF (1968) Tracing soil movement with fluorescent glass particles. Soil Sci Soc Am J 32:600–602

Zhang XC, Friedrich JM, Nearing MA, Norton LD (2001) Potential use of rare earth oxides as tracers for soil erosion and aggregation studies. Soil Sci Soc Am J 65:1508–1515

Zhang XC, Nearing MA, Polyakov VO, Friedrich JM (2003) Using rare-earth oxide tracers for studying soil erosion dynamics. Soil Sci Soc Am J 67:279–288